





Foresight and relaxation enable efficient control of nonlinear complex systems

Xin Zhang ¹, Xiaozhu Zhang ^{1,2}, Gang Yan ^{1,3,*} and Jack Murdoch Moore ^{1,3,†}

¹MOE Key Laboratory of Advanced Micro-Structured Materials, and School of Physical Science and Engineering, Tongji University, Shanghai, People's Republic of China

²Chair for Network Dynamics, Center for Advancing Electronics Dresden (cfaed)

and Institute for Theoretical Physics, Technical University of Dresden, 01062 Dresden, Germany

³National Key Laboratory of Autonomous Intelligent Unmanned Systems, and MOE Frontiers Science Center for Intelligent Autonomous Systems, Tongji University, Shanghai, People's Republic of China



(Received 9 May 2023; accepted 16 August 2023; published 29 August 2023)

There exist numerous effective techniques for influencing linear systems to desired outcomes, but control of general nonlinear complex systems remains an open problem. One promising technique, which exploits our deep understanding of linear systems, involves linearizing at the current position and then applying linear optimal control to move the system to a local target from which it should be easier to reach the desired final state. However, nonlocal trajectories are often required to influence linear systems even to local targets, meaning that local linearization-based strategies can lead to inefficient jagged trajectories with high path length and large control energy cost. To address these limitations, here we propose an alternative control strategy with two innovations. The first is avoiding fixation on varying local targets. Instead, we exercise foresight by consistently planning a complete route to the final target, moving a short distance along the planned route, and then updating the plan according to the new local conditions. The second refinement, which we term relaxation, discourages overinvestment in control strategies which are optimal according to the linearization at the current point but could be inefficient according to dynamical conditions encountered at later times. We evaluate our strategy on complex systems from neuroscience and statistical mechanics, showing that our innovations substantially increase the success rate of control for a given path length or energy expenditure, and that these advantages persist as system size increases.

DOI: [10.1103/PhysRevResearch.5.033138](https://doi.org/10.1103/PhysRevResearch.5.033138)

I. INTRODUCTION

Nonlinear differential equations coupled over complex networks can describe a wide range of important systems, including ecosystems [1], societies [2], metabolisms [3], and our own brains [4]. Because nonlinear complex systems such as these significantly impact human well being, there has been substantial interest in how they can be controlled [5–8]. While there exists a powerful suite of techniques for controlling linear systems, nonlinear control remains relatively undeveloped [9–12]. To control important systems towards better outcomes, we need versatile methods of nonlinear control.

One of the most popular means to investigate control of complex systems is to focus on linear dynamics upon complex topologies [13–23], or on a global linear approximation to the true nonlinear dynamics [24,25]. These studies have unveiled important impact of topological structure on system controllability and energy cost of control, yet such approaches could

be undermined by differences between linear and nonlinear systems [26,27]. There also exist methods which perform well in specific nonlinear contexts: the macroscopic states of some systems can be determined by fixing the state of a fraction of all nodes [28], another nonlinear control strategy can be applied when discontinuous perturbations can be applied to state variables [29], and feedback control can be an effective option for dissipative dynamical systems [30–32]. Here we focus on a promising local linearization-based strategy [17] involving a sequence of control inputs designed to minimize energy in driving the local linearization of the system to a nearby state from which it should be easier to reach the final target. Limitations of this approach arise because influencing systems to arbitrarily close local targets can require nonlocal control trajectories [33]. This invalidates the initial linear approximation and, as we will show, can lead to long, jagged trajectories and high control energy.

We propose two innovations to overcome the current limitations of local linearization-based control. The first of these is avoiding fixation on varying local targets. Instead, we exercise foresight and consistently plan a complete trajectory to the final target based on the linearization at the current point, apply control designed to advance an increment along this trajectory, and then evaluate the new local conditions before updating the planned route. The second is relaxation, which involves recognizing that the linearized system may be different at each point. Relaxation entails delaying energy expenditure

*gyan@tongji.edu.cn

†jackmoore@tongji.edu.cn

Published by the American Physical Society under the terms of the [Creative Commons Attribution 4.0 International](https://creativecommons.org/licenses/by/4.0/) license. Further distribution of this work must maintain attribution to the author(s) and the published article's title, journal citation, and DOI.

in directions which are currently unfavorable but which may be favorable according to the linearization at a future state. We apply our methods to complex systems from neuroscience and statistical mechanics, showing that across a wide range of conditions, our innovations substantially increase the rate of control success for a given path length or energy expenditure. Example code is available in Ref. [34].

II. BACKGROUND

In this section we introduce basic linear control theory and its application to nonlinear systems via local linearization.

A. Control of nonlinear systems

Consider a controlled nonlinear system evolving according to

$$\dot{\mathbf{x}}(t) = \mathbf{f}(\mathbf{x}(t)) + \mathbf{B} \cdot \mathbf{u}(t), \quad (1)$$

where $\mathbf{x}(t) \in \mathbb{R}^n$ is the state of the system, $\mathbf{f} : \mathbb{R}^n \rightarrow \mathbb{R}^n$ is a nonlinear vector field, $\mathbf{u}(t) \in \mathbb{R}^m$ is the control signal, \mathbf{B} is the $n \times m$ control matrix, and t is time. Given initial state \mathbf{x}_I and desired final state \mathbf{x}_F , we seek a control signal $\mathbf{u} : [t_I, t_F] \rightarrow \mathbb{R}^m$ such that the governing equation (1) and initial state $\mathbf{x}(t_I) = \mathbf{x}_I$ lead to the final state $\mathbf{x}(t_F) = \mathbf{x}_F$. A system is controllable when such a control signal \mathbf{u} exists for any choice of initial point \mathbf{x}_I , final point \mathbf{x}_F , initial time t_I , and final time $t_F > t_I$. Control signals $\mathbf{u} : [t_I, t_F] \rightarrow \mathbb{R}^m$ preferably correspond to low control times $t_F - t_I$, low path lengths

$$L = \int_{t_I}^{t_F} \|\dot{\mathbf{x}}(t)\| dt,$$

and low energies

$$E = \int_{t_I}^{t_F} \|\mathbf{u}(t)\|^2 dt.$$

In these expressions, $\|\cdot\|$ represents the Euclidean norm.

B. Control of linear systems

A controlled linear system evolves according to

$$\dot{\mathbf{x}}(t) = \mathbf{A} \cdot \mathbf{x}(t) + \mathbf{b} + \mathbf{B} \cdot \mathbf{u}(t), \quad (2)$$

where \mathbf{A} is the $n \times n$ system matrix, and $\mathbf{b} \in \mathbb{R}^n$ is a constant vector. Controllability of this system depends on the rank of the symmetric controllability Gramian for control over the time interval $t_I' \leq t \leq t_F'$, which is given by

$$\mathbf{W} = \int_{t_I'}^{t_F'} e^{\mathbf{A}(t_F' - \tau)} \mathbf{B} \mathbf{B}^T e^{\mathbf{A}^T(t_F' - \tau)} d\tau. \quad (3)$$

The system is controllable if and only if the Gramian \mathbf{W} is invertible, and in this case there exists an infinite number of control signals \mathbf{u} which can achieve the desired conditions $\mathbf{x}(t_I') = \mathbf{x}_I'$ and $\mathbf{x}(t_F') = \mathbf{x}_F'$ while also satisfying the governing equation (2). The particular control signal $\mathbf{u} : [t_I', t_F'] \rightarrow \mathbb{R}^m$ which minimizes the energy E is given by [10]

$$\mathbf{u}(t) = \mathbf{B}^T e^{\mathbf{A}^T(t_F' - t)} \mathbf{W}^{-1} \cdot (\mathbf{x}_F' - \mathbf{g}_F'), \quad (4)$$

where

$$\mathbf{g}(t) = e^{\mathbf{A}(t - t_I')} \cdot \mathbf{x}_I' + \int_{t_I'}^t e^{\mathbf{A}(t - \tau)} d\tau \cdot \mathbf{b} \quad (5)$$

is the free trajectory, which arises under Eq. (2) when $\mathbf{u} = \mathbf{0}$, and $\mathbf{g}_F' = \mathbf{g}(t_F')$. This control signal requires energy

$$E = (\mathbf{x}_F' - \mathbf{g}_F')^T \cdot \mathbf{W}^{-1} \cdot (\mathbf{x}_F' - \mathbf{g}_F'). \quad (6)$$

In practice, the control Gramian \mathbf{W} and free trajectory \mathbf{g} are usually determined by direct numerical integration of Eqs. (3) and (5), but this is computationally costly. As we explain in the Appendix, we instead employ the algebraic results presented in Ref. [35] to determine these quantities exactly and without numerical integration.

C. Control via linearization

Local linearization allows us to apply well-understood linear control methods to nonlinear systems. The linearization of Eq. (1) at $\mathbf{x} = \mathbf{x}_I'$ is Eq. (2) with

$$\mathbf{A} = \frac{\partial \mathbf{f}}{\partial \mathbf{x}}(\mathbf{x}_I'), \quad \mathbf{b} = \mathbf{f}(\mathbf{x}_I') - \mathbf{A} \cdot \mathbf{x}_I', \quad (7)$$

where $\frac{\partial \mathbf{f}}{\partial \mathbf{x}}(\mathbf{x}_I')$ is the Jacobian of \mathbf{f} at $\mathbf{x} = \mathbf{x}_I'$. To apply control for the linearization at $\mathbf{x}_I' = \mathbf{x}(t_I')$ with target position \mathbf{x}_F' at time t_F' we utilize the control input \mathbf{u} given by Eq. (4) in the definition of a controlled nonlinear system provided by Eq. (1). This is represented by the system

$$\begin{aligned} \dot{\mathbf{x}}(t) &= \mathbf{f}(\mathbf{x}(t)) + \mathbf{B} \mathbf{B}^T \cdot \mathbf{v}(t), \\ \dot{\mathbf{v}}(t) &= -\mathbf{A}^T \cdot \mathbf{v}(t), \end{aligned} \quad (8)$$

with initial condition

$$\begin{aligned} \mathbf{x}(t_I') &= \mathbf{x}_I', \\ \mathbf{v}(t_I') &= e^{\mathbf{A}^T(t_F' - t_I')} \mathbf{W}^{-1} \cdot (\mathbf{x}_I' - \mathbf{g}_F'), \end{aligned} \quad (9)$$

for which $\mathbf{u} = \mathbf{B}^T \cdot \mathbf{v}$ is the control input given by Eq. (4).

D. Local control strategies

The strategy of local linearization gave rise to the locally optimal control strategy (LOCS) [10], which involves a chain of steps of energy-minimising optimal control for the linearization at the current position, seeking each iteration to move closer to the desired final state \mathbf{x}_F . Because application of LOCS to a given nonlinear system requires tuning weight parameters based on prior knowledge of the system, we present two natural simplifications.

Energy-incrementing LOCS (EILOCS). Each iteration of EILOCS uses a fixed time increment $\Delta t = t_F' - t_I'$ and energy no more than a fixed increment ΔE . At the start of each iteration i we choose an immediate target \mathbf{x}_F' based on the current state $\mathbf{x}_i' = \mathbf{x}_{i-1}$, where the first current state is $\mathbf{x}_0 = \mathbf{x}_I$. If the energy

$$\Delta E_F = (\mathbf{x}_F - \mathbf{g}_F')^T \cdot \mathbf{W}^{-1} \cdot (\mathbf{x}_F - \mathbf{g}_F') \quad (10)$$

required to reach the final target \mathbf{x}_F according to the linearization at the current state \mathbf{x}_{i-1} satisfies $\Delta E_F \leq \Delta E$ then the initial target \mathbf{x}_F' is set to the final target \mathbf{x}_F . Otherwise, the intermediate target is chosen as

$$\mathbf{x}_F' = \mathbf{g}_F' + \sqrt{\frac{\Delta E}{\Delta E_F}} (\mathbf{x}_F - \mathbf{g}_F'), \quad (11)$$

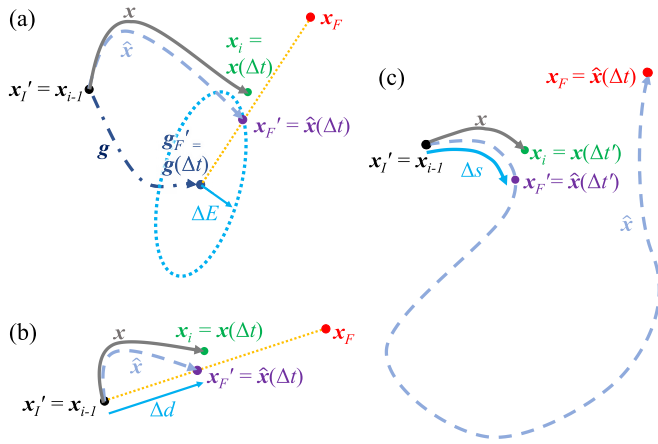


FIG. 1. We compare three control strategies based on local linearization. Iteration number i of three control strategies based on following the optimal trajectory \hat{x} according to the linearization at the current state $x_{i-1}' = x_{i-1}$. For simplicity, in this figure, we assume the time at the start of iteration i is $t_i' = 0$. [(a),(b)] Local control strategies representing simplifications of the established locally optimal control strategy (LOCS). (a) Energy-incrementing LOCS (EILOCS) seeks to use energy up to ΔE in a time step Δt to move directly towards the final target x_F from the destination $g_F = g(\Delta t)$ of the uncontrolled trajectory g . The pictured energy ellipsoid comprises all states which, according to the local linearization, can be reached in time Δt using energy ΔE . This includes the immediate target $x_F' = \hat{x}(\Delta t)$, where \hat{x} is the trajectory of the controlled linearized system. Applying the control signal leading to \hat{x} in the linear system leads to the trajectory x , which after time Δt reaches $x_i = x(\Delta t)$, which will be the starting point of the next iteration. (b) Distance-decrementing LOCS (DDLOCS) seeks to move up to distance Δd in a time step Δt to move directly in a straight line towards the final target x_F from the current state $x_{i-1}' = x_{i-1}$. (c) The proposed control strategy, arc length incrementation targeting endpoint (ALITE), aims to follow an optimal trajectory \hat{x} with target $\hat{x}(\Delta t)$ equal to the final target x_F . It seeks to follow this trajectory, not for the complete time Δt , but only for arc length Δs and time $\Delta t'$.

which is the point where the energy ellipsoid defined by Eq. (6) intersects the straight line from g_F' to x_F . We then apply optimal control for the linearization at the current state x_{i-1} with target x_i' . This brings the system to the new current state x_i and the end of iteration i . An iteration of EILOCS, for the case $\Delta E_F > \Delta E$, is illustrated in Fig. 1(a).

Distance-decrementing LOCS (DDLOCS). Each iteration of DDLOCS uses a fixed time increment $\Delta t = t_F' - t_i'$ and aims to bring the state up to distance decrement Δd closer to the final target x_F . At the start of each iteration i , if the final target x_F is within distance Δd of the current state x_{i-1} then we make the final target x_F our immediate target x_F' , i.e., we set $x_F' = x_F$. Otherwise, we choose as our immediate target x_F' the point

$$x_F' = x_{i-1} + \Delta d \frac{x_F - x_{i-1}}{\|x_F - x_{i-1}\|}, \quad (12)$$

which is distance Δd along the straight line from the current state x_{i-1} to the final target x_F . We then apply optimal control for the linearization at the current state x_{i-1} with target x_F' , which brings the system to the new current state x_i and the

end of iteration i . Figure 1(b) depicts an iteration of DDLOCS when $\|x_F - x_i\| > \Delta d$.

III. METHODS

In this section we present our proposed innovations to local linearization-based control of nonlinear complex systems, and describe our methods for comparing control strategies.

A. Foresight

Now we outline a way to incorporate global planning into control strategies without compromising the versatility of the local linearization approach. We exercise foresight by seeking to advance along the optimal control trajectory towards the final target according to the linearization at the current point, but only for a small distance Δs . After trying to cover this short distance, we identify the optimal control trajectory towards the final target based on the updated current position, and follow that instead.

Arc length incrementation targeting endpoint (ALITE). In each iteration we consider optimal control for the linearization at the current state x_{i-1} with target equal to the final target x_F . We then determine the length of time $\Delta t'$ after which the trajectory \hat{x} of the system linearized at the current state x_{i-1} under optimal control with target x_F will have traveled fixed arc length increment Δs , i.e., $\Delta t'$ such that

$$\Delta s = \int_{t_i'}^{t_i' + \Delta t'} \|\dot{\hat{x}}(t)\| dt.$$

Optimal control for the linearization at the current state x_{i-1} with target x_F is then applied for time $\Delta t'$, which brings the system to the new current state x_i at time $t_i' + \Delta t'$, and the end of iteration i . An iteration of ALITE is sketched in Fig. 1(c).

Figure 1 illustrates the main differences between ALITE and (EI/DD)LOCS. (1) From each distinct system state x_{i-1}' , LOCS aims for a different local target x_F' , while ALITE consistently seeks the final target x_F . (2) Under LOCS, control trajectories are determined by system displacements such as $x_F' - g_F'$ or $x_F' - x_{i-1}'$, which can be problematic when small displacements require nonlocal trajectories taking the system outside the region of validity of the local linearization. In contrast, ALITE considers distance along the predicted trajectory, and so can more effectively maintain validity of a linear approximation.

B. Relaxation

Here we indicate how an innovation we term relaxation can enhance control of nonlinear systems. Equation (10) reveals that the energy ΔE_F required to reach the final target x_F can be estimated based on linearization about the current state as

$$\Delta E_F = \sum_{j=1}^n \frac{y_j^2}{\mu_j} \mathbf{w}_j \cdot (x_F - g_F'),$$

where $\mu_1 \geq \mu_2 \geq \dots \geq \mu_n$ and $\mathbf{w}_1, \mathbf{w}_2, \dots, \mathbf{w}_n$ are the eigenvalues and corresponding orthonormal eigenvectors of the symmetric real Gramian matrix W and, for $j = 1, 2, \dots, n$, $y_j = (x_F - g_F')^T \cdot \mathbf{w}_j$ is the projection in the direction of \mathbf{w}_j of the difference $x_F - g_F'$ between the final

target \mathbf{x}_F and the system's destination \mathbf{g}_F' under free evolution. If $\mu_n \ll \mu_1$ then the predicted cost of moving the system in the direction of \mathbf{w}_1 is substantially greater than that of moving the system in direction \mathbf{w}_n .

Relaxation involves recognizing that the system is nonlinear and the Gramian W is constantly evolving. Therefore, at a later time it may be more energetically favorable to influence the system in the direction of the current \mathbf{w}_n . We avoid inefficient outlay of effort as simply as possible, by replacing the initial condition Eq. (9) with

$$\mathbf{v}(t_i') = e^{A^T(t_F' - t_i')} (W + p_i \bar{\mu} I)^{-1} \cdot (\mathbf{x}_i' - \mathbf{g}_F'), \quad (13)$$

where I is the $n \times n$ identity matrix, $\bar{\mu} = \frac{1}{n} \sum_{j=1}^n \mu_j$ is the mean of the eigenvalues of the Gramian [36] W , and $p_i \geq 0$ is the perturbation parameter in iteration i . The choice $p_i = 0$ corresponds to control without relaxation, while $p_i \rightarrow \infty$ corresponds to free evolution, without control. The initial condition Eq. (13) is equivalent to employing optimal control for the current state with target

$$\begin{aligned} \mathbf{g}_F' + W(W + p_i \bar{\mu} I)^{-1} \cdot (\mathbf{x}_i' - \mathbf{g}_F') \\ = \mathbf{g}_F' + \sum_{j=1}^n \frac{\mu_j}{\mu_j + p_i \bar{\mu}} y_j \mathbf{w}_j, \end{aligned}$$

which would incur energy cost

$$\Delta E_F' = \sum_{j=1}^n \frac{\mu_j}{(\mu_j + p_i \bar{\mu})^2} y_j^2.$$

The two preceding equations illustrate how relaxation reduces energy cost by delaying effort to influence the system in directions which currently appear energetically unfavorable. The further the distance between the final target \mathbf{x}_F and the state \mathbf{x}_{i-1} at the start of iteration i , the more remaining opportunity for variation the Gramian W will tend to have, and the larger the perturbation parameter p_i should be. Hence, the perturbation parameter p_i is chosen as

$$p_i = 2r \frac{\|\mathbf{x}_F - \mathbf{x}_{i-1}\|}{\|\mathbf{x}_F - \mathbf{x}_i\|},$$

where r is a constant we call the relaxation.

In Fig. 2 we illustrate control with and without relaxation for a five-dimensional neuronal system, which we will introduce in Sec. III C 1, and which has been slightly simplified such that its adjacency matrix $W = (w_{ij})$ is unweighted, with $w_{ij} \in \{0, 1\}$. We use ALITE to move the system from the initial point $\mathbf{x}_I = (-5.50, -3.50, -3.50, -5.50, -3.50)^T$ to the final target $\mathbf{x}_F = (5.50, 3.50, 3.50, 5.50, 3.50)^T$. If we use only the small value of relaxation $r = 10^{-6}$ then the system makes many sharp changes in the controlled variable x_3 as its state moves from \mathbf{x}_I to \mathbf{x}_F , increasing the total path length and energy cost. As the relaxation parameter r increases, the trajectory shortens and smooths, requiring lower control energy and exhibiting changes which are less abrupt.

In Fig. 3, considering the same slightly simplified neuronal system and relaxation $r = 10^{-4}$, we illustrate the limitations of EILOCS and DDLOCS which ALITE was developed to overcome. The strategies EILOCS and DDLOCS involve choosing a local target, but navigation to this nearby point

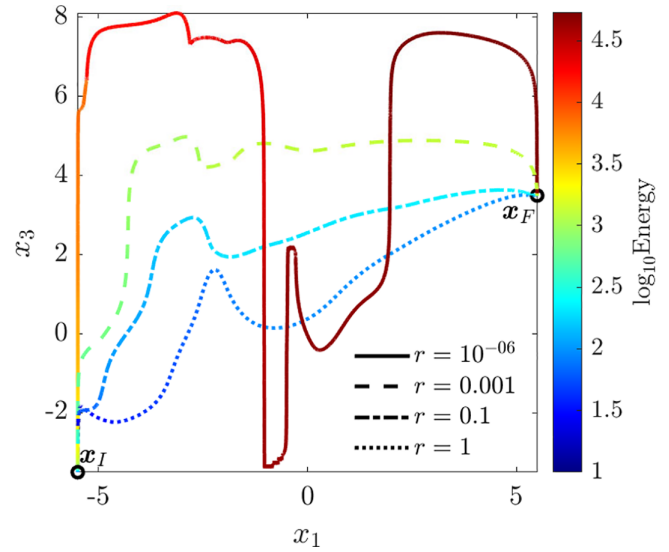


FIG. 2. Relaxation delays energy expenditure in directions which are currently energetically unfavorable. Using ALITE to drive a system from initial point \mathbf{x}_I to final target \mathbf{x}_F while controlling x_3 and x_5 . As the relaxation parameter r increases, the trajectory shortens and smooths, requiring changes in direction which are less sudden, and lower control energy. The color bar shows, at each point along the trajectory, the energy consumed so far.

can require a repetitively arching and nonlocal trajectory [33] requiring a substantial outlay of energy. Over successive iterations these build into an inefficient jagged path and high total energy cost. In contrast, by consistently planning and

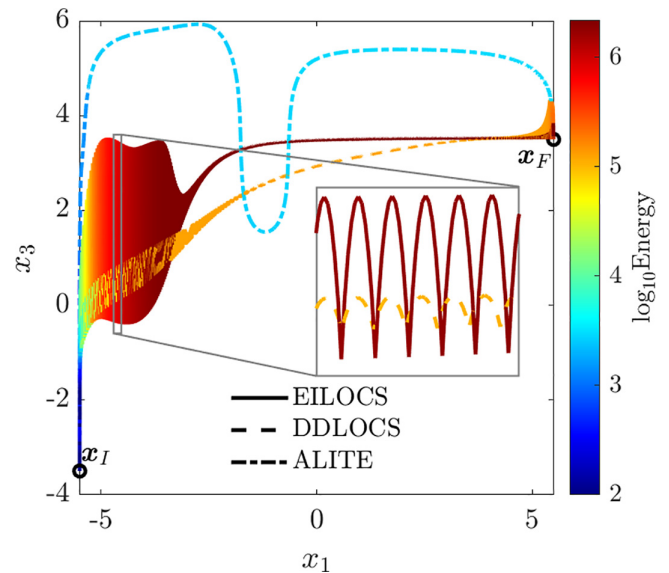


FIG. 3. Controlling the system towards local targets can induce oscillations which ALITE can avoid. Using control methods EILOCS, DDLOCS, and proposed strategy ALITE to drive a system from initial point \mathbf{x}_I to final target \mathbf{x}_F while controlling x_3 and x_4 . The color bar shows, at each point along the trajectory, the energy consumed so far. Inset: A portion of the trajectories arising under EILOCS and DDLOCS. We consider EILOCS with energy increment $\Delta E = 10^5$, which allows clear visualisation.

following an iteratively updated route to the final target, the proposed ALITE strategy can avoid this limitations, providing a smoother path and allowing lower energy expenditure.

C. Evaluation

In this section we delineate our approach for comparing different control strategies.

1. Considered systems

We evaluate our control strategy using two models. Drawing from neuroscience, we consider bistable neuronal systems [37] defined by

$$\frac{dx_i}{dt} = -x_i + s \tanh(x_i) + \sum_{j=1}^N w_{ij} \tanh(x_j),$$

where x_i describes the state of node i , which represents a local cluster of neurons, $W = (w_{ij})$ is the weighted adjacency matrix in which w_{ij} is the weighting of the edge from j to i , and $s = 1.5$ ($g = 2.0$) describes the strength of coupling within (between) clusters. From statistical mechanics we take diffusive spin systems [28] governed by

$$\frac{dx_i}{dt} = x_i(x_i + Q)(P - x_i) + g \sum_{j=1}^N w_{ij}(x_j - x_i),$$

where $P = 5$ and $Q = 1$ represent spin states.

These differential equations are coupled over random but fixed directed weighted networks (for examples see Supplemental Material (SM) [38], Fig. S1). In each network, 40% of edges (i, j) are bidirectional, with $w_{ij} = w_{ji}$, and the remainder are unidirectional, with either $w_{ij} = 0$ or $w_{ji} = 0$. Because self-dynamics appear elsewhere in the governing equations, diagonal terms are set to zero; $w_{ii} = 0$, $i = 1, 2, \dots, n$. Unless stated otherwise, nonzero weights w_{ij} are drawn independently from a Gaussian distribution with mean zero and standard deviation 0.2.

2. Control parameters

The considered control methods employ a total of five parameters: relaxation r , time increment Δt , energy increment ΔE , distance increment Δd , and arc length increment Δs . These are chosen to facilitate fair comparison of different methods. The time interval for EILOCS and DDLOCS is $\Delta t = \Delta t_0$, where the time increment Δt_0 can be thought of as an estimate of the time required to move Δd closer to the final target. For ALITE, the initial choice of time increment depends on distance to the final target according to $\Delta t = \Delta t_1 = \sqrt{\frac{\|\mathbf{x}_F - \mathbf{x}_I\|}{\Delta d}} \Delta t_0$, but is updated each iteration to reflect the remaining distance to the final target, according to

$$\Delta t = \sqrt{\frac{\|\mathbf{x}(t) - \mathbf{x}_I\|}{\|\mathbf{x}_F - \mathbf{x}_I\|}} \Delta t_1. \quad (14)$$

Distance and arc length increments are set equal, $\Delta s = \Delta d$.

We choose $\Delta d = \Delta s = 0.1$. For neuronal systems we use $\Delta t_0 = 10^{-2}$, and for spin systems we use $\Delta t_0 = 10^{-3}$. When using EILOCS, for neuronal systems we employ $\Delta E = 10^6$ unless stated otherwise, and for spin systems we choose

$\Delta E = 10^7$. These constitute favorable choices for each control method (see SM [38], Fig. S2). Relaxation r will be chosen to maximise the success rate for each combination of control strategy and type of dynamical system.

3. Scope

We consider the rate of success in controlling from one stable fixed point \mathbf{x}_I to a distinct stable fixed point \mathbf{x}_F . The five-dimensional neuronal system exhibits four stable fixed points, and we consider all twelve ordered pairs of distinct stable fixed points; for the five-dimensional spin system we identified twelve fixed points, and evaluate performance from twenty randomly chosen ordered pairs of distinct fixed points (for a list of the fixed points considered for each of these systems, see SM [38], Table S1). More generally, for a system with ν fixed points, among its $\nu(\nu - 1)$ ordered pairs of fixed points we consider $\min\{\nu(\nu - 1), 20\}$ randomly chosen ordered pairs of fixed points.

To reduce computational burden, for each ordered pair $(\mathbf{x}_I, \mathbf{x}_F)$ and for each control dimension $m = 1, 2, \dots, n$ we restrict ourselves to a single control set $\mathcal{C} = \{c_1, c_2, \dots, c_m\}$, where each control set \mathcal{C} corresponds to the diagonal control matrix $B = (b_{ij})$ for which $b_{ii} = \begin{cases} 1 & i \in \mathcal{C} \\ 0 & i \notin \mathcal{C} \end{cases}$. This control set is the subset of $\{1, 2, \dots, n\}$ of length m which maximises the minimum eigenvalue μ_n of the Gramian matrix W at the initial point \mathbf{x}_I when we take $t_F' - t_I' = \Delta t_0$. This constitutes a reasonable strategy for choosing control sets of a particular dimension (see SM [38], Fig. S3), but numerous other approaches exist [11,16,19]. We consider the minimum eigenvalue-maximising control set $\{c_1, c_2, \dots, c_m\}$ only when it provides structural controllability [39]; otherwise no control set of length m is considered.

Control is considered successful when it brings the system within Euclidean distance $d_{\max} = 10^{-3}$ of the final target \mathbf{x}_F within 10^4 iterations. The control attempt is also terminated if a recurrence is detected, which we consider to take place when the current state is within $10^{-5} \Delta t' \Delta d$ of a previous state, where $\Delta t'$ is the system time which passes in an iteration, i.e., the increase in the time variable t in the defining differential equations. ALITE is more sensitive than EILOCS or DDLOCS to the choice of d_{\max} (see SM [38], Fig. S4).

IV. RESULTS AND DISCUSSION

In this section, we show how the control strategies introduced above perform in controlling different systems. In Fig. 4 we show how the rate of successful control, energy cost, and required arc length vary with relaxation r for systems of $n = 5$ nodes. For each system and control method, the rate of success peaks for $r > 0$ [Figs. 4(a) and 4(d)]. For most combinations of system and control strategy, for a wide range of values of the relaxation r , the success rate is substantially higher than is the case without relaxation, i.e., for $r = 0$. These patterns demonstrate the value of relaxation in local linearization-based control of nonlinear complex systems. For the neuronal system, the highest success under DDLOCS is 92%, while EILOCS and the proposed method ALITE can achieve 100% control success. For the spin system, the highest success under EILOCS, DDLOCS, or ALITE is 71%. When

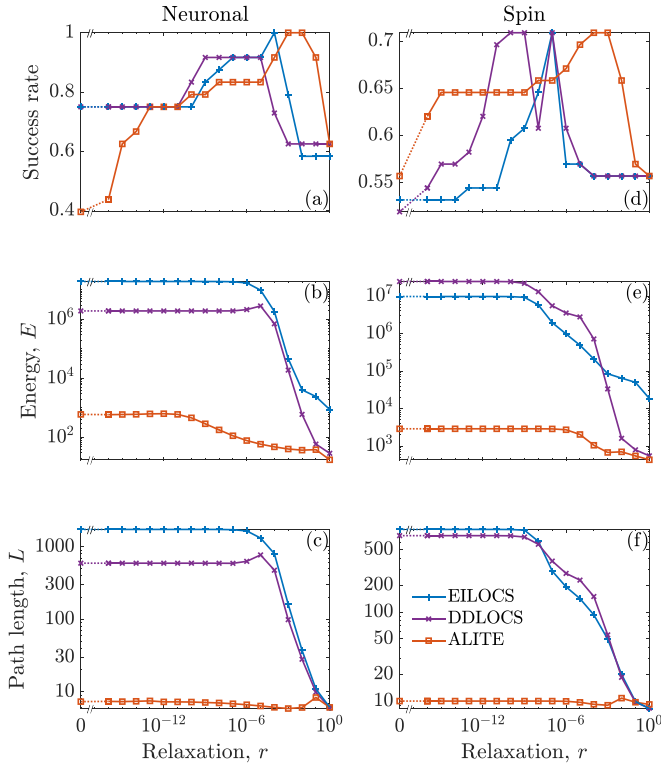


FIG. 4. Relaxation can increase the rate of success while decreasing the required control energy and arc length. Rate of success, arc length, and control energy versus relaxation r for control methods EILOCS and DDLOCS, and proposed strategy ALITE. For (a)–(c) neuronal system, and (d)–(f) spin system, variation with relaxation r of [(a),(d)] success rate; [(b),(e)] required control energy E ; and [(c),(f)] arc length L . For fair comparison, (b), (c), (e), and (f) the mean across pairs of fixed points for which control was successful for all considered control strategies and rates of relaxation r .

we consider the neuronal (spin) system, the largest values of r for which peak success occurs are $r = 10^{-4}$, 10^{-5} , and 10^{-2} ($r = 10^{-7}$, 10^{-7} , and 10^{-3}) for EILOCS, DDLOCS, and ALITE respectively, and it is these values we use in subsequent control experiments. For each system and control strategy, energy and arc length requirements at the optimal relaxation are consistently less than for $r = 0$ [Figs. 4(b), 4(c), 4(e), and 4(f)]. More generally, energy and arc length tend to decrease as relaxation r grows, although path length under ALITE can exhibit a slight increase around the largest r considered. Across a wide range of values of the relaxation r , ALITE requires energy and arc length substantially less than EILOCS or DDLOCS.

To gain further understanding of how energy and path length efficiency vary with control strategy, in Fig. 5 we consider, for each system and each control method, how the rate of success varies with the maximum energy, path length or time we can afford to expend in controlling the system. After a short interval of low energies and path lengths for which performance can be similar, EILOCS and DDLOCS require orders of magnitude more resources to match the performance of ALITE. For example, to achieve 45% success for neuronal (spin) dynamics, ALITE requires about 100 units (1000 units)

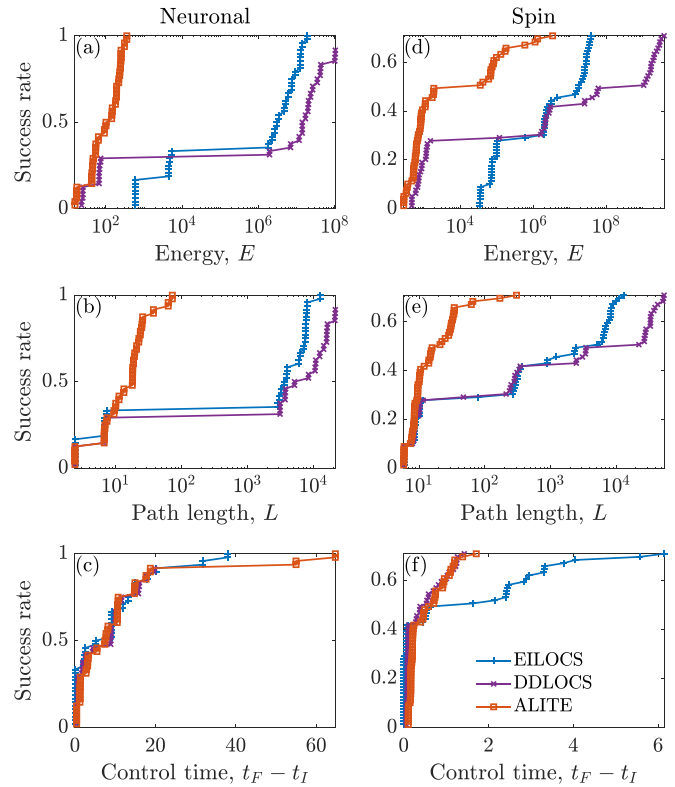


FIG. 5. The proposed control strategy decreases the energy and path length required for successful control. Rate of success for control methods EILOCS and DDLOCS and proposed strategy ALITE. For (a)–(c) neuronal system; and (d)–(f) spin system, success vs required: [(a),(d)] energy; [(b),(e)] arc length; and [(c),(f)] control time.

of energy while EILOCS and DDLOCS require about 3×10^6 and 10^7 units (3×10^6 and 3×10^7 units) respectively. The advantages of ALITE in terms of path length are similar to those for energy, but differences in required control time are less. Perhaps counterintuitively, the method EILOCS can sometimes achieve control success with energy less than the energy increment ΔE . This requires that according to the linearization at \mathbf{x}_I , navigation to the final point \mathbf{x}_F within a single-time increment Δt requires energy less than ΔE .

We have demonstrated that both relaxation and ALITE are valuable for controlling model systems of dimension $n = 5$ from both neuroscience and statistical mechanics. Now we show that the advantages of our innovations extend to higher dimension. In Fig. 6 we show how the rate of successful control depend on the total number n of neurons in the system and on the number m of neurons which are accessible to control. As system size increases from $n = 1$ up to $n = 20$ neurons, the rate of success under EILOCS and DDLOCS fluctuates at around 60% [Fig. 6(a)]. The proposed strategy ALITE maintains a higher rate of success, which fluctuates at about 70%. For systems of $n = 20$ neurons, the proposed strategy ALITE allows success when controlling fewer nodes than EILOCS or DDLOCS. ALITE can achieve over 50% success when controlling only six neurons, and achieves a perfect rate of success as long as 12 or more neurons are controlled [Fig. 6(d)]. In contrast, EILOCS and DDLOCS require access

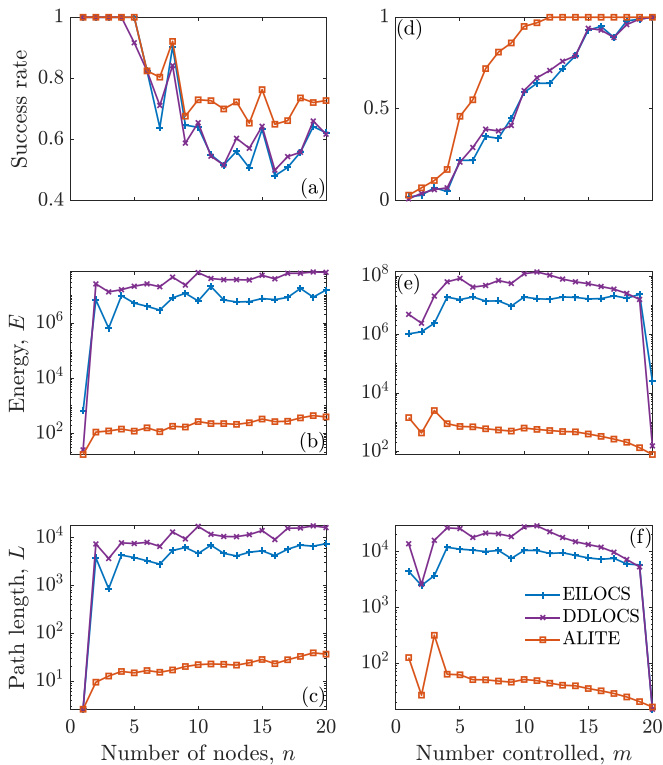


FIG. 6. The proposed control strategy increases success rate across a range of system sizes and controllability conditions. Rate of success for neuronal system controlled using EILOCS, DDLOCS, and proposed method ALITE. Rate of success vs: (a) total number of nodes n ; and (b) number of controlled nodes for fixed system size $n = 20$. In (b) we show the mean over five independently generated networks. For fair comparison, (b), (c), (e), and (f) show the mean across control between pairs of fixed points for which control was successful for all control strategies at the considered value of n [m].

to 10 neurons to guarantee at least 50% success, and do not achieve 100% success unless all 20 neurons are controlled. Across a wide range of values of system size n or control dimension m , ALITE requires energy and arc length substantially less than EILOCS or DDLOCS [Figs. 6(b), 6(c), 6(e), and 6(f)]. This finding is corroborated by Fig. 7, which shows

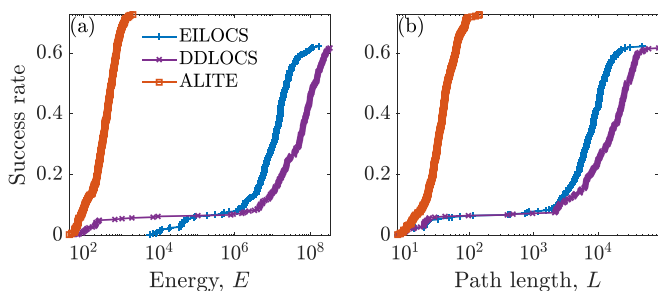


FIG. 7. The proposed control strategy decreases the energy and path length required for successful control of higher-dimensional systems. Rate of success for control methods EILOCS and DDLOCS and proposed strategy ALITE in controlling a system of $n = 20$ neurons. Rate of success achieved within maximum allowed: (a) energy; and (b) arc length.

how the rate of success varies with the maximum energy, path length, or time we can afford to expend in controlling a system of $n = 20$ neurons. The figure reveals that at this higher system size, ALITE has even clearer advantages in terms of energy and path length than were apparent for $n = 5$ (see Fig. 5). ALITE can also be used to influence a system of $n = 200$ neurons via direct access to only half of these entities (see SM [38], Fig. S4).

V. CONCLUSIONS

Methods for controlling networked nonlinear systems are needed to improve the outcomes from important real-world complex systems. A promising approach, based on seeking nearby points based on linearization at the current point, is undermined by the fact that trajectories which move a system to a local target are not necessarily local. In this paper, we propose a method of control by local linearization which mitigates this issue by: (1) Exercising foresight by avoiding fixation on varying nearby targets and instead using local conditions to plan a complete route to the final target; and (2) accommodating the changing energy landscape via an innovation we term relaxation, which delays energy expenditure in directions which are currently energetically unfavorable but which may be convenient from a later system state. By considering complex systems from neuroscience and statistical mechanics and with a range of system sizes, we showed that our innovations substantially increase the efficiency of control via local linearization in terms of path length or energy expenditure.

The ALITE method was developed with utility in mind. As a control strategy based on local linearization, ALITE can be applied wherever derivatives of the governing dynamics can be calculated or estimated numerically. To plan its next iteration, our control strategy utilizes only the linearization at the current point; information which may be easier to access than the global nonlinear dynamics or even the exact nonlinear dynamics in a local region. Control is open loop within each iteration, requiring only a measurement of each state rather than a continuously applied feedback loop, which will make it easier to implement ALITE in real time. The smoother and shorter trajectories provided by ALITE and relaxation will help to keep the system bounded in a region in which it is well understood and avoid wild excursions to mysterious territories in which the utilized dynamical model is less valid. This is in contrast to other forms of local linearization-based control such as EILOCS and DDLOCS. ALITE and relaxation also facilitate the reduction in control energy which is a recurring goal in control theory. Furthermore, relaxation mitigates computational challenges and could help to improve numerical controllability.

A valuable direction for future research would be applying ALITE to search for fundamental patterns and scaling laws in the controllability properties of nonlinear complex systems [40,41]. We have shown that relaxation is an effective method of controlling path length, but it is somewhat indirect. Therefore, it would be useful to implement and explore versions of ALITE which plan trajectories by minimizing objective functions representing, not only energy, but also other important properties such as path length. Temporal network

variation which is predictable and independent of system state corresponds to advantages for control [18,21], but our consistent reliance on local system properties implies uncertainty, which can challenge control strategies [42]. Our addition of a relaxation term provided a simple way to ameliorate this uncertainty, but more sophisticated control strategies could arise from combining knowledge of variation in local linearizations with the stochastic temporal network control framework of Ref. [42].

ACKNOWLEDGMENTS

This work was supported by the National Natural Science Foundation of China (Grants No. T2225022, No. 12150410309, No. 12161141016, and No. 11875043), Shuguang Program of Shanghai Education Development Foundation and Shanghai Municipal Education Commission (Grant No. 22SG21), Shanghai Municipal Science and Technology Major Project (Grant No. 2021SHZDZX0100), Shanghai Municipal Commission of Science and Technology Project (Grant No. 19511132101), and the Fundamental Research Funds for the Central Universities. We thank Michael Small for useful discussion.

APPENDIX: FAST CALCULATION OF CONTROL GRAMIAN AND FREE TRAJECTORY

In this Appendix we illustrate how the control Gramian W and free trajectory \mathbf{g} can be determined rapidly, exactly, and without numerical integration, based on the results of Ref. [35]. The control Gramian W given by Eq. (3) can be written as

$$W = \int_{t_i'}^{t_F'} e^{-A's} Q e^{A^T s} ds,$$

where $A' = -A^T$ and $Q = e^{A(t_F - t_i')} B B^T e^{A^T(t_F - t_i')}$ is a symmetric matrix. Hence, by Eqs. (1.2) and (2.2) of Ref. [35], the Gramian W is given by

$$W = F_3^T G_3,$$

where

$$e^{C_1} = \begin{pmatrix} F_2 & G_2 \\ O & F_3 \end{pmatrix}, \quad C_1 = \begin{pmatrix} -A'^T & Q \\ O & A' \end{pmatrix},$$

F_2, G_2, F_3 are $n \times n$ matrices, and O is the $n \times n$ zero matrix.

To determine the final state $\mathbf{g}_{F'}$ of the free trajectory \mathbf{g} we must compute the integral which appears in Eq. (5) at the final time t_F . As long as A is invertible we have

$$\int_{t_i'}^{t_F'} e^{A(t-\tau)} d\tau = A^{-1}(I - e^{A(t_i - t)}),$$

where I is the $n \times n$ identity matrix. The integral can also be calculated while avoiding matrix inversion by expressing it as

$$\int_{t_i'}^{t_F'} e^{A(t_F - \tau)} d\tau = \int_0^{t_F' - t_i'} e^{As} ds.$$

Equations (1.1) and (2.1) of Ref. [35] therefore imply

$$\int_{t_i'}^{t_F'} e^{A(t_F - \tau)} d\tau = G_3$$

where

$$e^{C_2} = \begin{pmatrix} F_3 & G_3 \\ O & F_4 \end{pmatrix}, \quad C_2 = \begin{pmatrix} A & I \\ O & O \end{pmatrix}.$$

[1] J. Gao, B. Barzel, and A.-L. Barabási, Universal resilience patterns in complex networks, *Nature (London)* **530**, 307 (2016).

[2] P. Ji, J. Ye, Y. Mu, W. Lin, Y. Tian, C. Hens, M. Perc, Y. Tang, J. Sun, and J. Kurths, Signal propagation in complex networks, *Phys. Rep.* **1017**, 1 (2023).

[3] N. M. Mangan, S. L. Brunton, J. L. Proctor, and J. N. Kutz, Inferring biological networks by sparse identification of nonlinear dynamics, *IEEE Trans. Mol. Biol. Multi-Scale Commun.* **2**, 52 (2016).

[4] V. L. Galinsky and L. R. Frank, Collective Synchronous Spiking in a Brain Network of Coupled Nonlinear Oscillators, *Phys. Rev. Lett.* **126**, 158102 (2021).

[5] S. Wuchty, Controllability in protein interaction networks, *Proc. Natl. Acad. Sci. USA* **111**, 7156 (2014).

[6] R. Albert, J. Baillieul, and A. E. Motter, Introduction to the special issue on approaches to control biological and biologically inspired networks, *IEEE Trans. Control Netw. Syst.* **5**, 690 (2018).

[7] C. W. Lynn and D. S. Bassett, The physics of brain network structure, function and control, *Nat. Rev. Phys.* **1**, 318 (2019).

[8] X. Li, X. Wang, and G. Chen, Pinning a complex dynamical network to its equilibrium, *IEEE Trans. Circuits Syst. I: Regul. Pap.* **51**, 2074 (2004).

[9] A. J. Whalen, S. N. Brennan, T. D. Sauer, and S. J. Schiff, Observability and Controllability of Nonlinear Networks: The Role of Symmetry, *Phys. Rev. X* **5**, 011005 (2015).

[10] I. Klickstein, A. Shirin, and F. Sorrentino, Locally Optimal Control of Complex Networks, *Phys. Rev. Lett.* **119**, 268301 (2017).

[11] Y.-Y. Liu and A.-L. Barabási, Control principles of complex systems, *Rev. Mod. Phys.* **88**, 035006 (2016).

[12] R. M. D'Souza, M. di Bernardo, and Y.-Y. Liu, Controlling complex networks with complex nodes, *Nat. Rev. Phys.* **5**, 250 (2023).

[13] G. Yan, J. Ren, Y.-C. Lai, C.-H. Lai, and B. Li, Controlling Complex Networks: How Much Energy Is Needed? *Phys. Rev. Lett.* **108**, 218703 (2012).

[14] M. Pósfai and P. Hövel, Structural controllability of temporal networks, *New J. Phys.* **16**, 123055 (2014).

[15] J. Gao, Y.-Y. Liu, R. M. D'Souza, and A.-L. Barabási, Target control of complex networks, *Nat. Commun.* **5**, 5415 (2014).

[16] F. Lo Iudice, F. Garofalo, and F. Sorrentino, Structural permeability of complex networks to control signals, *Nat. Commun.* **6**, 8349 (2015).

[17] I. Klickstein, A. Shirin, and F. Sorrentino, Energy scaling of targeted optimal control of complex networks, *Nat. Commun.* **8**, 15145 (2017).

- [18] A. Li, S. P. Cornelius, Y.-Y. Liu, L. Wang, and A.-L. Barabási, The fundamental advantages of temporal networks, *Science* **358**, 1042 (2017).
- [19] G. Lindmark and C. Altafini, Minimum energy control for complex networks, *Sci. Rep.* **8**, 3188 (2018).
- [20] J. Z. Kim, J. M. Soffer, A. E. Kahn, J. M. Vettel, F. Pasqualetti, and D. S. Bassett, Role of graph architecture in controlling dynamical networks with applications to neural systems, *Nat. Phys.* **14**, 91 (2018).
- [21] X.-Y. Zhang, J. Sun, and G. Yan, Why temporal networks are more controllable: Link weight variation offers superiority, *Phys. Rev. Res.* **3**, L032045 (2021).
- [22] H. Chen and E. H. Yong, Energy cost study for controlling complex social networks with conformity behavior, *Phys. Rev. E* **104**, 014301 (2021).
- [23] C. Duan, T. Nishikawa, and A. E. Motter, Prevalence and scalable control of localized networks, *Proc. Natl. Acad. Sci. USA* **119**, e2122566119 (2022).
- [24] M. T. Angulo, C. H. Moog, and Y.-Y. Liu, A theoretical framework for controlling complex microbial communities, *Nat. Commun.* **10**, 1045 (2019).
- [25] G. Baggio, D. S. Bassett, and F. Pasqualetti, Data-driven control of complex networks, *Nat. Commun.* **12**, 1429 (2021).
- [26] H. Nijmeijer and A. Van der Schaft, *Nonlinear Dynamical Control Systems*, Vol. 175 (Springer, New York, 1990).
- [27] E. D. Sontag, *Mathematical Control Theory: Deterministic Finite Dimensional Systems*, Vol. 6 (Springer Science & Business Media, New York, 2013).
- [28] H. Sanhedrai, J. Gao, A. Bashan, M. Schwartz, S. Havlin, and B. Barzel, Reviving a failed network through microscopic interventions, *Nat. Phys.* **18**, 338 (2022).
- [29] S. P. Cornelius, W. L. Kath, and A. E. Motter, Realistic control of network dynamics, *Nat. Commun.* **4**, 1942 (2013).
- [30] B. Fiedler, A. Mochizuki, G. Kurosawa, and D. Saito, Dynamics and control at feedback vertex sets. I: Informative and determining nodes in regulatory networks, *J. Dyn. Differ. Equ.* **25**, 563 (2013).
- [31] A. Mochizuki, B. Fiedler, G. Kurosawa, and D. Saito, Dynamics and control at feedback vertex sets. II: A faithful monitor to determine the diversity of molecular activities in regulatory networks, *J. Theor. Biol.* **335**, 130 (2013).
- [32] J. G. T. Zañudo, G. Yang, and R. Albert, Structure-based control of complex networks with nonlinear dynamics, *Proc. Natl. Acad. Sci. USA* **114**, 7234 (2017).
- [33] J. Sun and A. E. Motter, Controllability Transition and Non-locality in Network Control, *Phys. Rev. Lett.* **110**, 208701 (2013).
- [34] J. M. Moore, control-with-foresight, <https://github.com/JackMurdochMoore/control-with-foresight> (2022).
- [35] C. Van Loan, Computing integrals involving the matrix exponential, *IEEE Trans. Autom. Control* **23**, 395 (1978).
- [36] For readability, we suppress time and iteration dependence of variables including the Gramian W .
- [37] M. Stern, H. Sompolinsky, and L. F. Abbott, Dynamics of random neural networks with bistable units, *Phys. Rev. E* **90**, 062710 (2014).
- [38] See Supplemental Material at <http://link.aps.org/supplemental/10.1103/PhysRevResearch.5.033138> for additional figures and a table supporting our results.
- [39] S. Pequito, S. Kar, and A. P. Aguiar, A framework for structural input/output and control configuration selection in large-scale systems, *IEEE Trans. Autom. Control* **61**, 303 (2015).
- [40] G. Yan, G. Tsekenis, B. Barzel, J.-J. Slotine, Y.-Y. Liu, and A.-L. Barabási, Spectrum of controlling and observing complex networks, *Nat. Phys.* **11**, 779 (2015).
- [41] J. M. Moore, G. Yan, and E. G. Altmann, Nonparametric Power-Law Surrogates, *Phys. Rev. X* **12**, 021056 (2022).
- [42] P. De Lellis, A. Di Meglio, F. Garofalo, and F. Lo Iudice, The inherent uncertainty of temporal networks is a true challenge for control, *Sci. Rep.* **11**, 6977 (2021).